Supplemetary Materials for Stress Drop Variations in the Region of the 2014 M_W8.1 Iquique Earthquake, Northern Chile

J. Folesky[1], J. Kummerow[1], S.A. Shapiro[1]
[1] Freie Universität Berlin, Department of Geophysics, Berlin, Germany
Corresponding author: jonas.folesky[at]geophysik.fu-berlin.de

May 5, 2020

Influence of Smoothing on the Corner Frequency Estimates

We test the influence of the Konno-Omachi smoothing on the estimated corner frequency. For this, the spectra of an EGF pair are simulated using the Boatwright spectral model with input parameters $\Omega_1, fc_1, \Omega_2, fc_2$ in the range of typical values from the real data. White random noise is added such that the noise amplitude is stable over all frequencies. Noise range is ± 0.5 times the model amplitude of the smaller event. The spectra are then smoothed using the konnoohmachismoothing function from Obspy an implementation of the approach of Konno and Ohmachi, 1998. Next, the ratio of the two spectra is computed and the data is fitted using the trust region reflective method from scipy curve_fit. In Figure 1, ten exemplary event pair curves are shown. The procedure is iterated for different fc_1 values with 1000 runs for each tested corner frequency. The results, shown in Table 1, demonstrate that the input parameters are recovered reliably. The standard deviation values are in the range of 15%. A minimal systematic shift towards smaller values for fc_1 is seen. We conclude that the systematic shift of fc_1 can be neglected for real

fc_{in}	fc_{out}	fc_{std}
4	4.0	0.7
7	6.9	0.9
10	9.8	1.2
14	13.5	1.9

Table 1: Results of synthetic smoothing tests for 1000 iterations using varying input values for the corner frequency fc_1 in Hz. All other inputs are fixed ($\Omega_1 = 100, fc_1 = var, \Omega_2 = 10, fc_2 = 25$).

data and that the smoothing is applicable.

Description of Resulting Stress drop Table

File name: stress_drop_tbl_NChile.txt

Columns are: Event origin time, latitude, longitude, depth, moment magnitude, corner frequency, stress drop, number of contributing data traces, internal ID

Origin time, latitude, longitude, depth are taken from Sippl et al. 2018

Moment magnitudes are taken from Münchmeier et al. 2020

Note, that internal ID is given up to 2 times. First occurrence is the P phase, second is the S phase based estimate.

Important! Note, that P phase based stress drops have been computed with k_p=0.32 and S phase based stress drop estimates have been computed with k_s = 0.25, resulting from Figure 2, main manuscript.

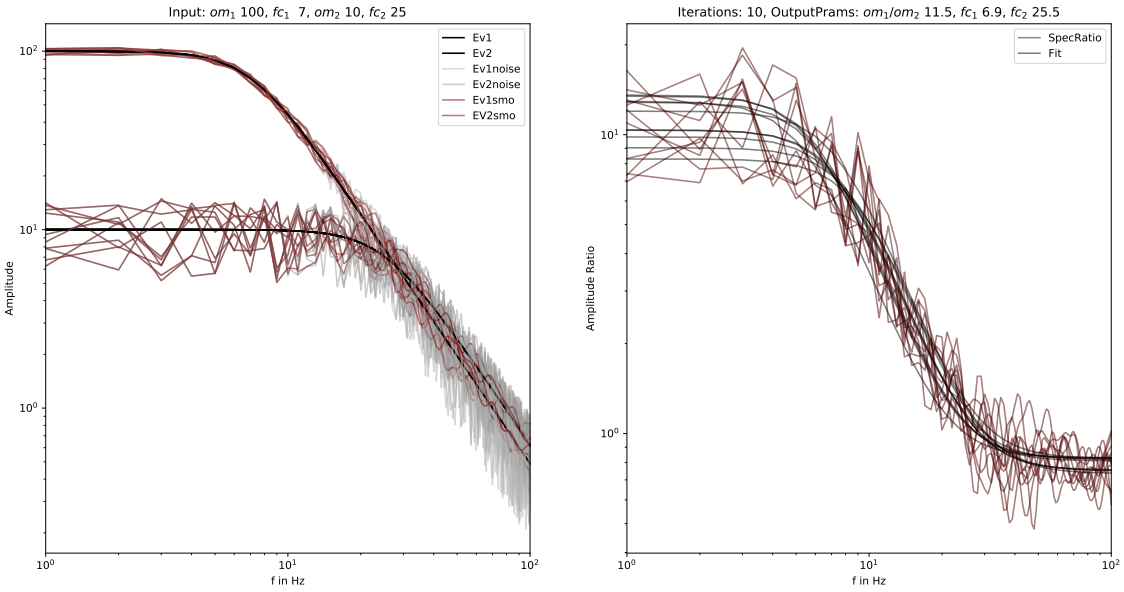

Figure 1: Influence of smoothing [Konno and Ohmachi, 1998] on the estimated corner frequency. Displayed are ten realizations of the test. On the left the input spectra, the spectra with noise and the smoothed spectra of the target and of the EGF event are shown. On the right the corresponding spectral ratios are shown with their fits, respectively. The input and output parameters are displayed above the plots. The smoothing operator has only a minimal impact on the decrease of the estimated corner frequency. We conclude that it is reasonable to use the approach to stabilize the spectral ratio approach with the real data.

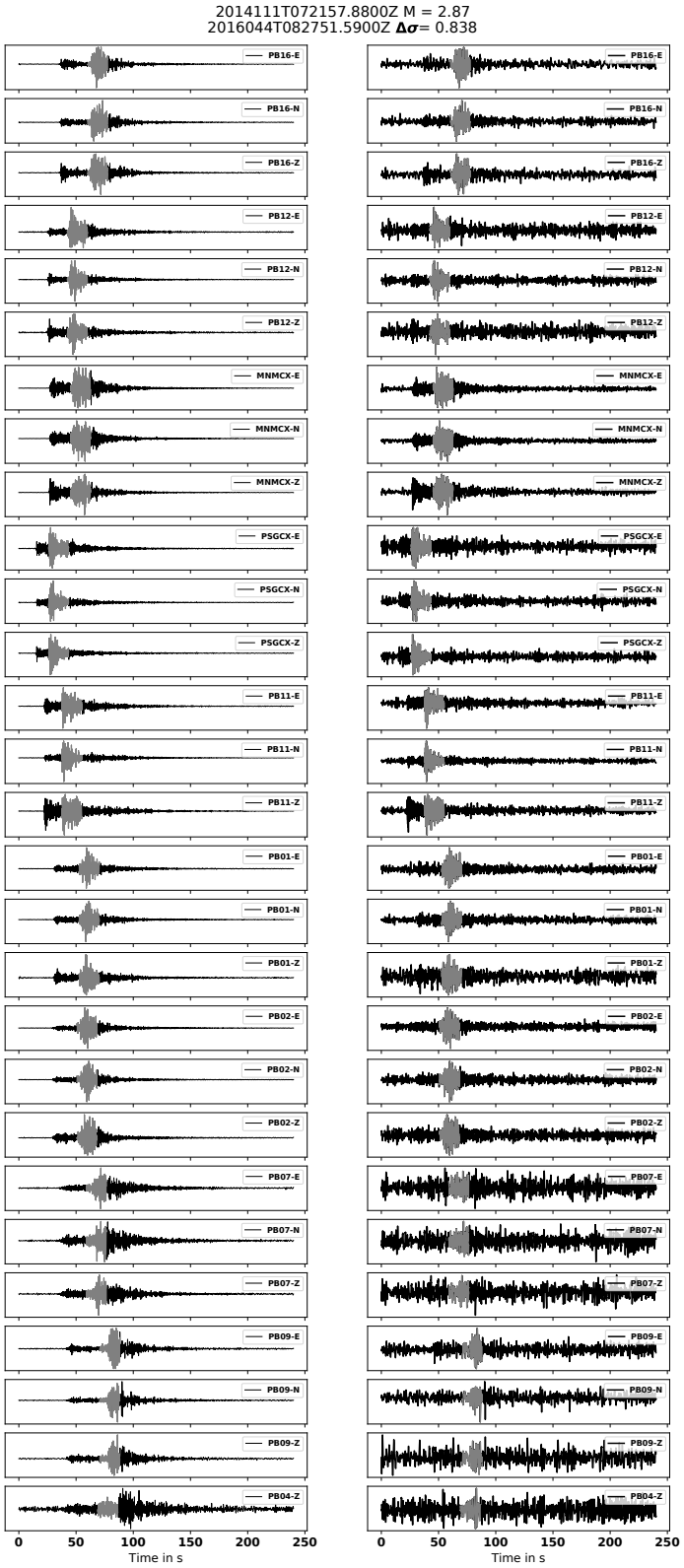

Figure 2: Selected S phase windows for an exemplary event pair. On the left the target event is shown, on the right, the EGF partner with the smaller magnitude.

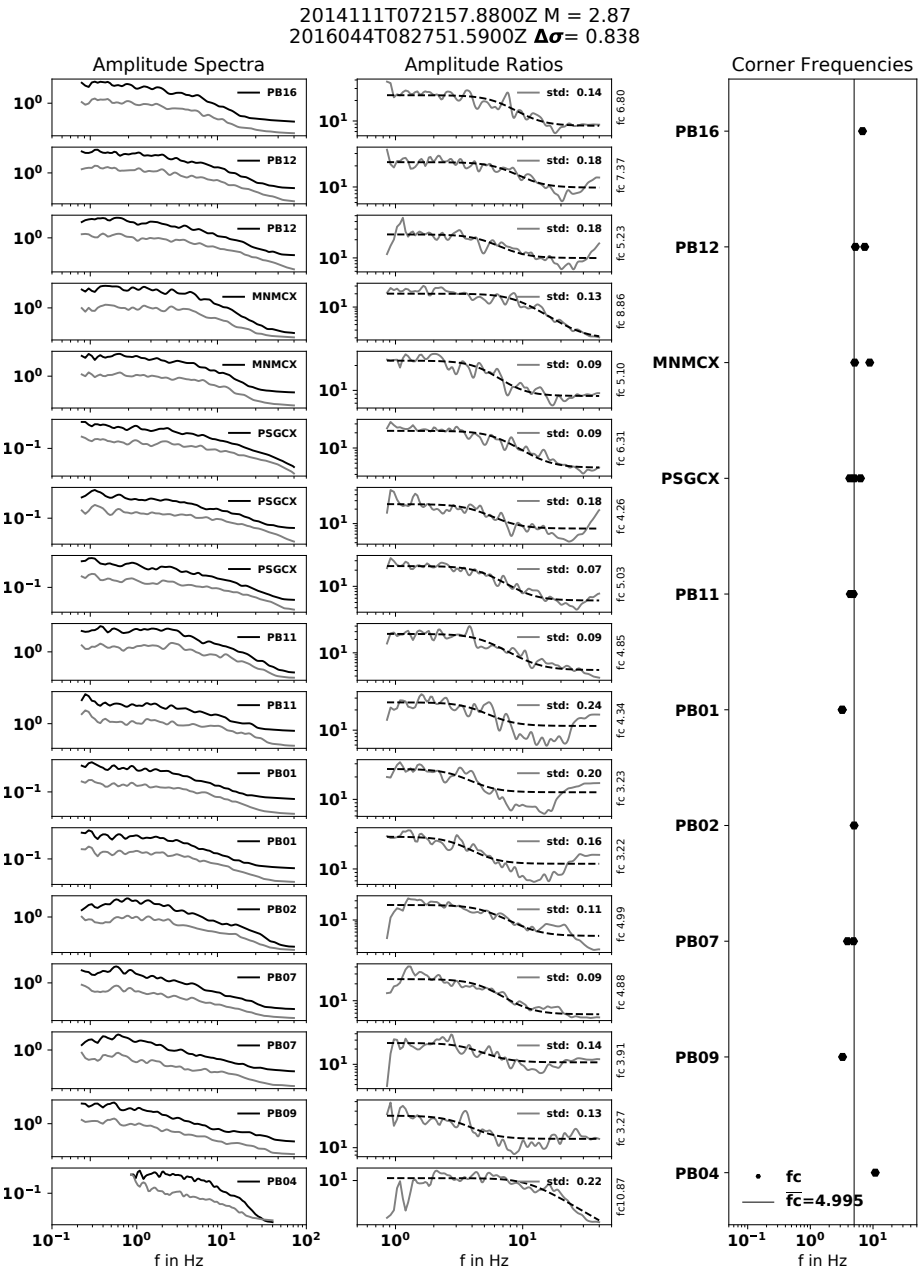

Figure 3: Left: Smoothed source spectra of the event pair from Figure 2. Center: The spectral ratio and the Boatwright spectral model fit. Right: Station wise corner frequencies with median value. Station sorting is north to south.

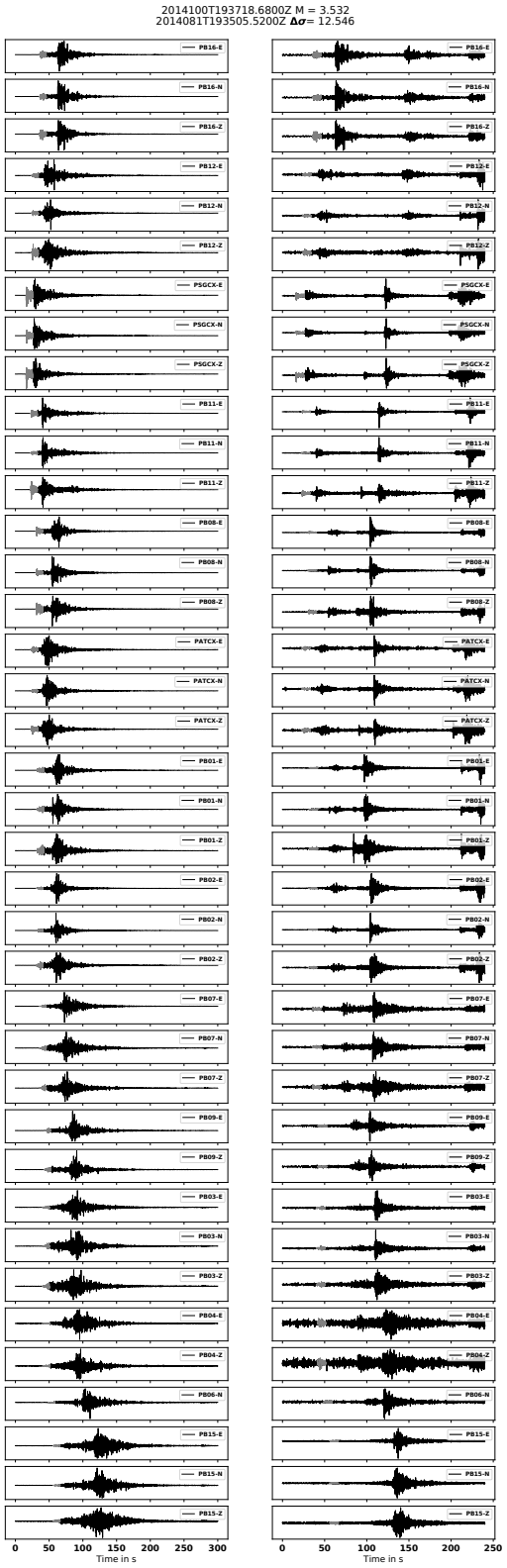

Figure 4: Selected P phase windows for an exemplary event pair. On the left the target event is shown, on the right, the EGF partner with the smaller magnitude.

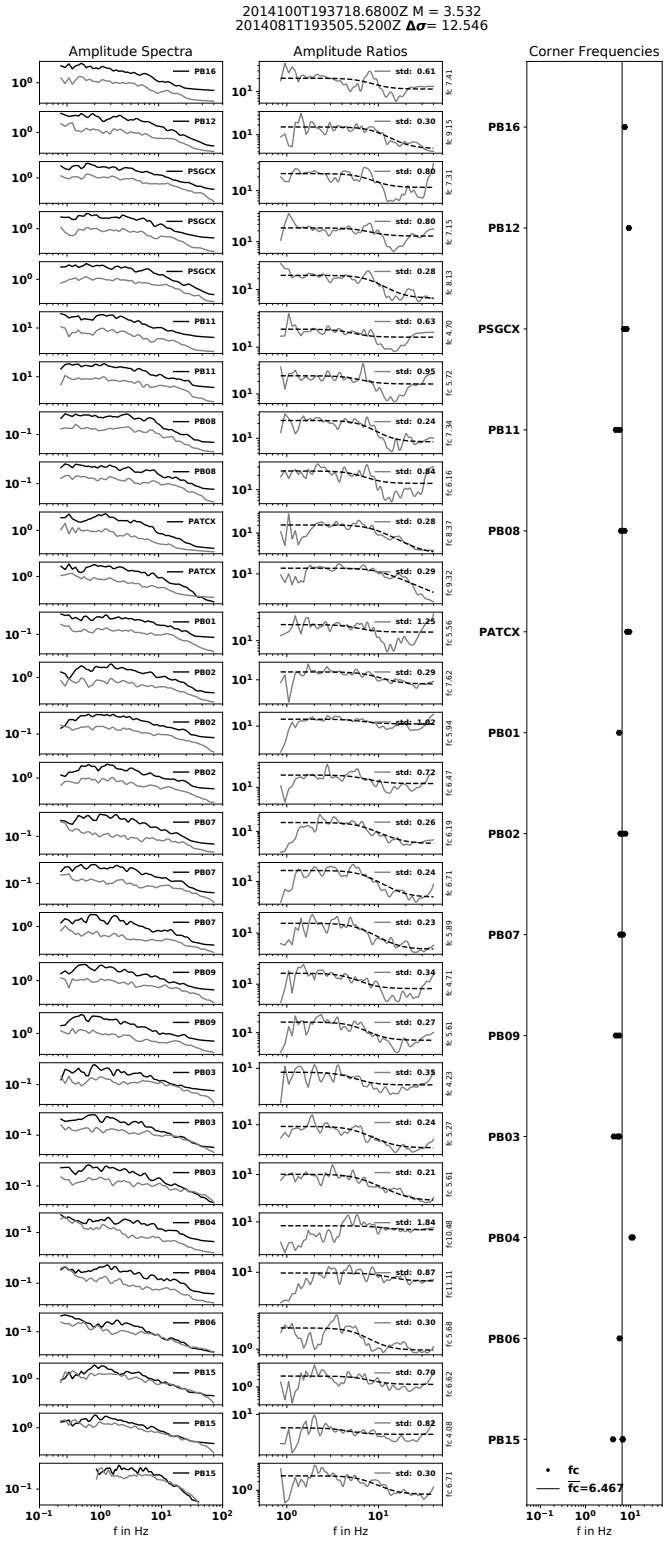

Figure 5: Left: Smoothed source spectra of the event pair from Figure 4. Center: The spectral ratio and the Boatwright spectral model fit. Right: Station wise corner frequencies with median value. Station sorting is north to south.

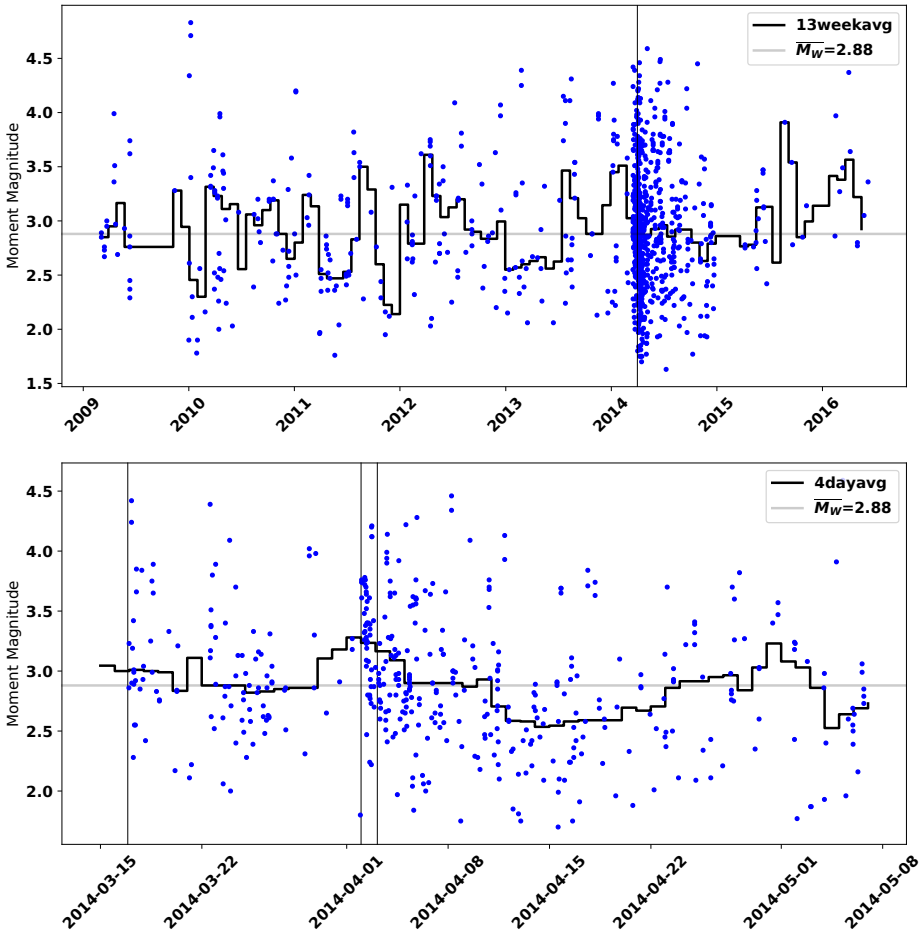

Figure 6: Variation of event magnitude with time. The figure shows the same time intervals as used for the temporal stress drop variation (Figure 9 main manuscript). The three vertical grey lines in the bottom panel denote the origin times of the M_W6.6 foreshock, the M_W8.1 mainshock, and the M_W7.6 aftershock. In both panels the median magnitude of the entire result ensemble ($M_W = 2.88$) is underlain as a grey line. Note the principally similar behavior of the curves compared to the stress drop curves in Figure 9 of the main manuscript. The shapes of the two curves show similarity indicating a correlation of event moment magnitude and stress drop which is substantiated in Figure 10 of the main manuscript.

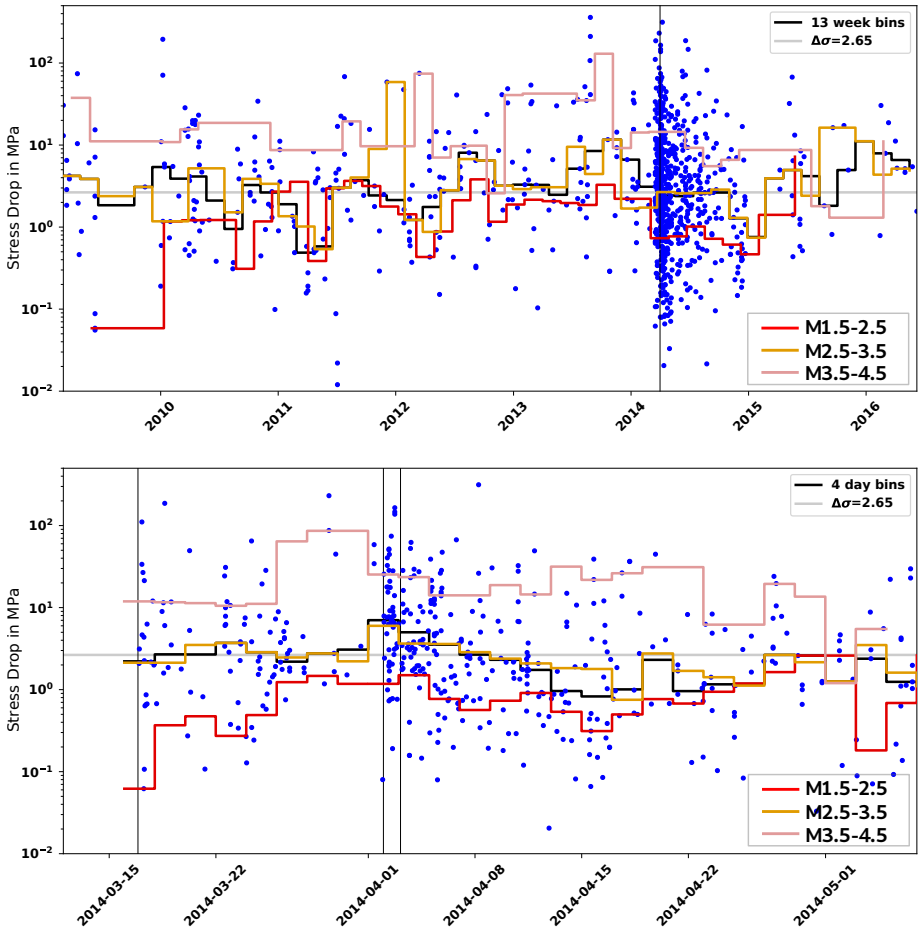

Figure 7: Magnitude dependent stress drop variation in the time domain corresponding to Figure 6 from the supplement and Figure 9 from the main manuscript. The black line is the median stress drop for bins of 13 weeks in top and 4 days in bottom panel, both for all included event magnitudes. The colored lines represent the same binned median stress drop but are confined to three different magnitudes ranges. Note that while small variations of each line vary individually the overall behavior of the curves is similar, especially the rise prior to the main event followed by a decline of median values to a minimum after which the curves rise again to their average values.